



Copolymers of a novel amphiphilic methacrylate monomer based on the hydroxyl group: copolymerization kinetics, thermal properties, biological activity, and swelling behavior

İbrahim Erol¹ · Murat Özer¹

Received: 16 March 2021 / Accepted: 16 August 2021 / Published online: 10 September 2021
© The Polymer Society, Taipei 2021

Abstract

In this work, in a first step, a novel methacrylate monomer, 2-(4-hydroxyanilino)-2-oxoethyl-2-methylprop-2-enoate (HAOEME), was synthesized containing a phenolic hydroxyl group in the side branch. Then, the copolymers of this monomer were obtained by a free radical solution polymerization method with glycidyl methacrylate (GMA), a commercial monomer, at 65 °C in 1,4-dioxane solvent. The structural characterization of the synthesized monomers and copolymers was carried out using Fourier transform infrared (FTIR) spectroscopy, proton nuclear magnetic resonance (¹H NMR), and ¹³C NMR techniques. Based on the monomer reactivity ratios obtained, the HAOEME monomer was found to be more reactive than GMA. The thermogravimetric analysis results showed that the thermal resistance of copolymers increased with an increase in the number of HAOEME units in the copolymer. It was also observed that the T_g value of copolymers increased with an increase of the molar fraction of HAOEMA units in the copolymer. The thermal degradation activation energy values of the polymers were determined using approaches including the Kissinger and Ozawa methods. The result of the biological activity studies revealed that the copolymers show moderate activity against different bacterial and fungal species. The swelling properties of the polymers were investigated using water. The variations in the swelling percentages were examined according to time and temperature parameters.

Keywords Amphiphilic · Antimicrobial activity · Monomer reactivity ratios · Phenolic hydroxyl · Methacrylate

Introduction

Functional polymers are used in different fields for various applications. Further application areas can be created, especially in polymeric structures, thanks to modifications on the minor or main chain, such as promoter in organic synthesis and catalysis [1, 2]. Some types of polymers are used in medical applications [3].

Our research group has conducted many studies on the synthesis and characterization of new polymers. In recent years, it has been especially focused on the modification of methacrylate monomers and polymers with different functional groups and their copolymerization with commercial monomers [4–7]. Homopolymers and copolymers

of methacrylates are used widely in industry and medicine. Functional methacrylates are used for various applications depending on the reactivity of the group they carry. A biocompatible polymer molecule can be used as a biological agent due to its degradation properties in tissue and urine [8, 9]. Methacrylate polymers have good optical clarity and are therefore called organic glass. They have a wide variety of applications due to their high light absorption, mechanical tolerance, and thermal resistance.

Over the past three decades, the use of amphiphilic polymers has been of great interest in a number of applications [10]. In addition, amphiphilic copolymer types that can respond to environmental stimuli can be added to biosensors, innovative drug delivery systems, and bioimaging, which have attracted much attention in the last few years [11–13]. Polymeric materials based on amphiphilic copolymers have recently been used for the production of pesticide formulations. As a result, research on the synthesis and characterization of amphiphilic block copolymers has increased tremendously. This is due to their unusual molecular composition,

✉ İbrahim Erol
ierol@aku.edu.tr

¹ Department of Chemistry, Faculty of Science and Arts, University of Afyon Kocatepe, Afyonkarahisar, Turkey

consisting of at least two distinct chemical properties, which have an amphiphilic character. The general features of amphiphilic polymers consist of a hydrophobic (water-insoluble) chain and a hydrophilic (water-soluble) chain [14]. It is also clear that methacrylate copolymers are a biocompatible matrix for tissue engineering [15, 16]. Polyhydroxyethyl methacrylate and its copolymers are known to be biocompatible and create the best alternatives for biomedical applications [17].

Glycidyl methacrylate (GMA) is a reactive monomer with a convertible epoxy group enabling various functionalizations through the epoxy ring-opening. The reaction of the epoxy group with different nucleophilic reagents containing thiol [18], hydroxyl [19], carboxyl [20], or amine groups [21] is one way to modify poly(GMA) chemically. Furthermore, poly(GMA) is a very versatile polymer that has been used in adhesives [22], surface coatings [23], super absorbents [24], composites [25], bioreactors [26], and drug delivery systems [27].

Knowledge regarding the specific properties of copolymers is essential in determining the areas of use. The microstructure of copolymers varies according to the reactivity ratio of the monomers. The most widely validated mathematical method of copolymerization is determining the parameters that will allow the computation of monomer-reactivity ratios using the relationship between the copolymer combination and the monomer start mixture [28, 29]. To calculate the monomer-reactivity ratio, the molar fractions in the initial and copolymer composition of the monomers used must be known. It is possible to calculate the reactivity ratios (r_1 and r_2) by determining the copolymer composition through spectroscopic approaches such as $^1\text{H-NMR}$ and $^{13}\text{C-NMR}$ [30, 31] or methods such as elemental analysis.

Thermogravimetric analysis (TGA) has been widely used for many years to determine the thermal resistance of many polymeric materials. The data obtained by TGA can be used to determine the material's kinetic parameters [32, 33].

This study synthesized a new amphiphilic methacrylate monomer, 2-(4-hydroxyanilino)-2-oxoethyl-2-methylprop-2-enoate (HAOEME), carrying a phenolic hydroxyl group in the side branch. Next, we prepared the copolymers based on the novel methacrylate monomer (HAOEME) and GMA monomer through free radical solution polymerization. HAOEME is a new amphiphilic methacrylic monomer with a side chain phenolic hydroxyl group. To the best of our knowledge, a similar methacrylate structure does not exist in the literature.

The synthesis of a novel methacrylic monomer containing a phenolic hydroxyl group and copolymerization of this monomer with an essential commercial monomer such as GMA is a subject of interest for polymer chemistry. This manuscript aimed to define the kinetics of radical copolymerization of the new HAOEME monomer with GMA,

calculate the monomer reactivity ratios, and investigate the thermal behavior, swelling properties, and biological properties of the obtained copolymers. The results are discussed in detail, and the relationship between structure and activity is revealed.

Materials and methods

Materials

Methacryloyl chloride, chloroacetyl chloride, sodium methacrylate, and 4-aminophenol (Sigma) were used as obtained. Ethanol, methanol, chloroform, n-hexane, and benzene were freshly purified in molecular sieves before use. 1,4-Dioxane, acetonitrile, and potassium carbonate (Sigma) were used as obtained. Azobisisobutyronitrile (AIBN) was recrystallized from a mixture of chloroform and methanol (v/v: 1/3). No further purification was necessary, as all other chemicals were of analytical quality.

Characterization techniques

The Fourier transform infrared spectroscopy (FTIR) spectra of the molecules were measured with the Shimadzu IRAffinity-1S FTIR spectrometer. Proton nuclear magnetic resonance ($^1\text{H NMR}$) and $^{13}\text{C NMR}$ spectra were obtained using a Bruker DPX 400 MHz spectrometer with tetramethylsilane as standard and CDCl_3 as solvent. An Elementar CHNS elemental analyzer was used to determine the ratio of N in the copolymer. The molecular weights (M_w and M_n) of the polymers were determined using gel permeation chromatography (Waters 410, Canada) equipped with a differential refractive index detector and calibrated with polystyrene standards. The thermal stability of the polymers was determined using a Shimadzu DSC 60H thermogravimetric analyzer/differential scanning calorimeter under inert N_2 (99.99% purity). Measurements were obtained from room temperature up to 500 °C at a heating rate of 20 °C/min⁻¹. The polymeric sample weighing about 5–8 mg was packed in an aluminum pan, and the measurements were made at a gas flow of 5 L/h⁻¹.

Synthesis of HAOEME monomer

Monomer synthesis was carried out in two steps.

In the first step, the 4-aminophenol compound was reacted with chloroacetyl chloride as described in the literature and the 2-chloro-N-(4-hydroxyphenyl)acetamide compound was prepared [34].

In the second step, 1 mmol of 2-chloro-N-(4-hydroxyphenyl)acetamide and 1.1 mmol of sodium methacrylate were mixed in 100 ml acetonitrile at 75–80 °C in

a reflux condenser for 24 h, and 2-(4-hydroxyanilino)-2-oxoethyl-2-methylprop-2-enoate (HAOEME) monomer was obtained. After the reaction, the mixture was cooled and filtered, and the solvent was removed by evaporation. The monomer obtained was purified by crystallization of ethanol (yield 80%).

The synthesized monomer was characterized by FTIR and ^1H and ^{13}C -NMR spectra.

1-IR (KBr pellet), cm^{-1} ; 3,100 (Ar-H stretch.); 1,680 and 1,722 (C=O of amide and ester); 3,214 (-NH stretch.); 1,635 (-C=CH₂); 1,254 (C-O-C); 2,990 (Alip. C-H).

2- ^1H NMR (δ , ppm from TMS in DMSO): 6.8–7.5 (Ar-H, 4H); 5.6 (CH₂=, 1H); 6.2 (CH₂=, 1H); 1.9 (CH₃-, 3H), 4.8 (OCH₂, 2H), 10 (NH, 1H), 3,3 (OH, 1H).

3- ^{13}C NMR (δ , ppm from TMS in DMSO): 164 and 168 (two C=O carbonyl of amide and ester); 138 (=C); 126 (CH₂=); 114–155 (Ar-C); 18 (CH₃ α -methyl on monomeric unit).

Synthesis of Poly(HAOEME)

The HAOEME monomer was polymerized using the free radical solution polymerization method. The polymerization reaction was achieved in a solution of 1,4-dioxane with AIBN (1% by total weight of monomers) as an initiator in N₂ atmosphere in glass ampoules at 65 °C in an oil bath. The homopolymer was obtained by precipitation in ethanol. The polymers that were precipitated and dried for purification purposes were re-dissolved from CH₂Cl₂ solution, and their precipitation was performed in ethanol. The resulting homopolymer was dried to a constant weight in a vacuum oven at room temperature.

Copolymerization

Considering the previously calculated monomer compositions, poly(HAOEME-co-GMA) copolymers were prepared by radical solution polymerization in an inert N₂ environment. This was carried out at 65 °C using AIBN (1% of the total weight of monomers) as an initiator in 1,4-dioxane solvent in the system. The determined amounts of HAOEME and GMA monomers were mixed in 1,4-dioxane in a polymerization tube and degassed with N₂ for 20 min. The tube was then allowed to copolymerize at 65 °C in an oil bath. Conversions were kept around 10%. Copolymer samples obtained were precipitated in ethanol. The polymers obtained were dissolved in 1,4-dioxane again for purification and precipitated in ethanol. The copolymers obtained in the final step were dried at 70 °C in a vacuum oven for 12 h. The composition of resulting copolymers was determined with elemental analysis (N content of HAOEME units).

Determination of the monomer reactivity ratios

Using the Fineman–Ross (F-R) [35] and Kelen–Tüdös (K-T) [36] methods, we calculated the monomer reactivity ratio. For this purpose, we prepared copolymers with different monomer compositions and low conversions. The composition of the copolymers was determined by elemental analysis. F-R and K-T parameters were calculated using the following equations:

$$F = M_1/M_2$$

$$f = m_1/m_2$$

$$H = F^2/f$$

$$G = F(f - 1)/f$$

$$\eta = G/(a + H)$$

$$\xi = H/(a + H)$$

$$a = (H_{max} \cdot H_{min})^{1/2}$$

Reactivity ratio r_1 and r_2 values were calculated by substituting them in their formulas. Here, M_1 and M_2 are molar fractions of the monomers in the mixture, and m_1 and m_2 are the molar fractions in the copolymer composition.

The K-T method equation is below:

$$\eta = (r_1 + r_2/\alpha)\xi - r_2/\alpha \quad (1)$$

K-T parameters were calculated using the starting monomer and copolymer composition monomer ratios. From these calculated parameters, η and ξ were plotted on a graph. From the graph, the η value for $\xi = 0$ is r_2/α .

$$\text{The F - R method equation is } G = Hr_1 - r_2 \quad (2)$$

The calculated G and H values were plotted on a graph. The graph gives a line equation. The slope of the G–H line is r_1 , and its shift corresponds to the value of r_2 .

Antimicrobial activity of the polymers

The antimicrobial effects of the poly(HAOEMA) and copolymers on various microorganisms were investigated in DMSO solution at two different concentrations (50 and 100 μg). To do this, *Staphylococcus aureus* ATCC 29,213, *Escherichia coli* ATCC 25,922, *Pseudomonas aeruginosa* ATCC 27853, *Proteus vulgaris*, *Salmonella enteritidis*, and *Klebsiella pneumoniae* were used as bacteria, and *Candida albicans* CCM 31 as fungus. A medium cell culture of yeast extract peptone dextrose (YEPD) was prepared according to

the methods in the literature [37]. A solid medium (Mueller Hinton agar [MHA]) suitable for the microorganism was prepared and poured into petri dishes to examine its antibiotic sensitivity. The turbidity of the 24-h liquid microorganism culture was adjusted to 0.5 McFarland. A swab was dipped into the liquid culture and kept there until the culture was thoroughly absorbed. The microorganism cultivation was carried out by rubbing the swab on the culture petri surface at an angle of 120°. The process was carried out at least six times to spread the microorganisms onto the entire petri dish. Antibiotic discs were placed on the surface of the implanted petri dish, depending on the size of the petri dish, and lightly pressed with forceps. The petri dish with antibiotic discs was incubated at the temperature and time (37 °C, 24 h) the microorganism would be able to grow. The biocidal susceptibility of the polymers was investigated as determined in the antibiotic disc test [38], and these prepared antibiotic disks (50 and 100 µg) were settled on the outer surface of the agar medium [39]. After incubation, the transparent inhibition zones formed on the surface of the petri dish around the disc were measured in millimeters. We compared the measured value with the standard values, and the activity of the microorganism against bacteria was determined. This proved that when an inactive material is released from the disc, bacterial growth around the sample is inhibited. The width of this region refers to the diffusion of the antimicrobial effect.

Standard deviation (SD) values of the detected biological activity results were calculated. SD is a measure of how far each data point in a study group deviates from the mean—in other words, how wide the distribution is. Defined another way, the indication of how wide (or narrow) a range a studied trait (or particularly relevant values or measurements) is distributed in a given population is the variance and the standard deviation, which is its derivative. By comparing the values obtained from the test statistics with the two or one end of the probability density function of our theoretical distribution, *p* values were obtained. This value gives the probability that the difference between variables is by chance. The mean ± standard deviation (SD) values of the results were determined by one-way analysis of variance using SPSS software (IBM Corp, Armonk, NY, USA), where the level of significant difference was determined as *p* < 0.05.

Swelling

The swelling properties of the polymers were investigated using the gravimetric method considering time and temperature parameters. In the first step, the polymer samples in pressed disc form were weighed and allowed to swell in a buffer solution (pH = 7) for 72 h at room temperature. The swollen polymers, which were taken from the swelling medium at certain times, were carefully dried with filter

paper. The reweighed polymers were placed in the same bath. The same procedure was carried out for each polymer sample until it reached a constant weight. The percent swelling (%S) values were calculated according to Eq. 3. All results were accepted as the mean value of three repeated measurements.

$$S(\%) = \frac{m_w - m_d}{m_d} \times 100 \quad (3)$$

where m_w is the wet weight of the sample and m_d is the dry weight of the sample before swelling.

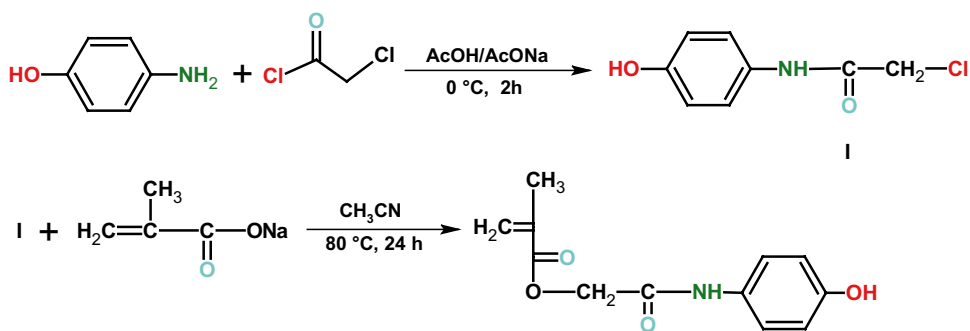
In the second step, the effect of temperature on the swelling behavior of polymers was investigated. For this purpose, the dried and weighed polymers were allowed to swell in a buffer solution (pH = 7) at different temperatures ranging from 30 to 70 °C. After 36 h, the swelling samples were removed, carefully dried with filter paper, and weighed. The %S values were calculated according to Eq. 3. All results were accepted as the mean value of three repeated measurements.

Results and discussion

The synthesis of phenolic hydroxyl-based methacrylate monomer was carried out in two steps. First, 2-chloro-N-(4-hydroxyphenyl)acetamide intermediate (I) was obtained by acylation reaction of chloroacetyl chloride with 4-aminophenol. Second, the target methacrylate monomer was obtained by a nucleophilic substitution reaction of 2-chloro-N-(4-hydroxyphenyl)acetamide with sodium methacrylate in acetonitrile. Based on the spectroscopic data obtained from the ¹H NMR and ¹³C NMR techniques, it appears that the synthesized phenolic hydroxyl-based methacrylate monomer conforms to the chemical structure shown in Scheme 1.

Characterization of the HAOEME and its homopolymer

Figure 1 shows the important peaks in the FTIR spectrum of the HAOEME monomer. There was a good match between structure and spectrum. In the FTIR spectrum of poly(HAOEME), the most prominent peak was the stretching vibrations of the ester and amide carbonyl groups at 1640 and 1724 cm⁻¹, and the OH stretching vibration bands at 3500 cm⁻¹. The stretching vibration bands belonging to N–H groups were observed at approximately 3300 cm⁻¹. During the polymerization process, the (C=C) peaks seen at 1635 cm⁻¹ were lost, and the ester carbonyl stretching vibration bands shifted to approximately 1742 cm⁻¹. One of the most important results of our study is that some typical signals of double bonds disappeared with polymerization.

Scheme 1 Synthesis of HAOEME monomer

These were the absorption peak at 921 cm^{-1} of the C-H bending of geminal $=\text{CH}_2$ and the C=C stretching vibration bands at 1605 cm^{-1} . The disappearing peaks represent the characteristic $-\text{C}=\text{CH}_2$ structure belonging to the vinyl monomeric structure, and as a result of polymerization, this structure turns into a $-\text{C}-\text{CH}_2$ structure containing single bonds.

The ^1H and ^{13}C NMR spectra of poly(HAOEME) characterized the structure significantly. The disappearance of the two vinyl protons at 5.6 and 6.2 ppm in the ^1H NMR spectrum and the presence of a broad peak at 1.2 and 2.1 ppm of the new aliphatic protons were indicative of the formation of polymers. The peak changes with polymerization were observed in the proton-decoupled ^{13}C NMR spectrum of poly(HAOEME). The signals at 165 and 169 ppm are attributed to two carbonyl groups (amide and ester) in the polymeric structure. Signals belonging to the polymeric α -methyl group were observed at 14 ppm. Signals of aromatic carbons were detected between 120 and 160 ppm. Figure 2 shows the ^1H NMR spectrum of poly(HAOEME).

Characterization of the copolymers

The monomeric components of the copolymer can be seen in Scheme 2.

Spectroscopic characterization

FTIR spectrum

The FTIR spectrum of a copolymer sample shown in Fig. 3 is in good agreement with the structure. The NH and OH stretching vibration bands of HAOEME units in the copolymer appear as a flat peak at approximately 3500 cm^{-1} . This is due to the dense H bonds between the HAOEME and the GMA unit in the copolymer. The absorption band at 3080 cm^{-1} is assigned to the C-H stretching vibration bands belonging to the aromatic groups. Ester stretching vibration bands in the HAOEME and GMA units appear as broad peaks at approximately 1737 cm^{-1} . The amide carbonyl absorption band in the HAOEME units is found at

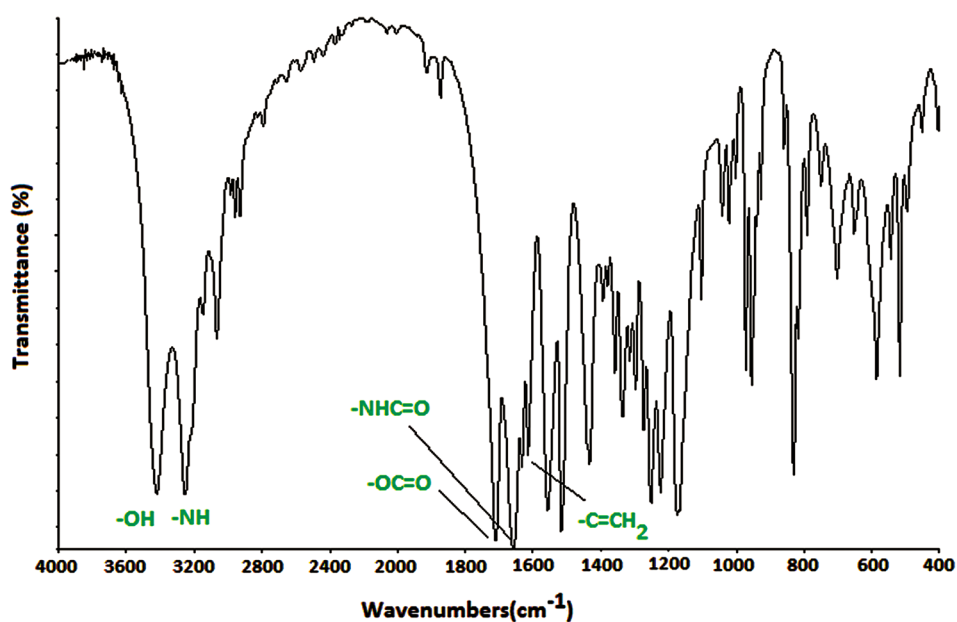
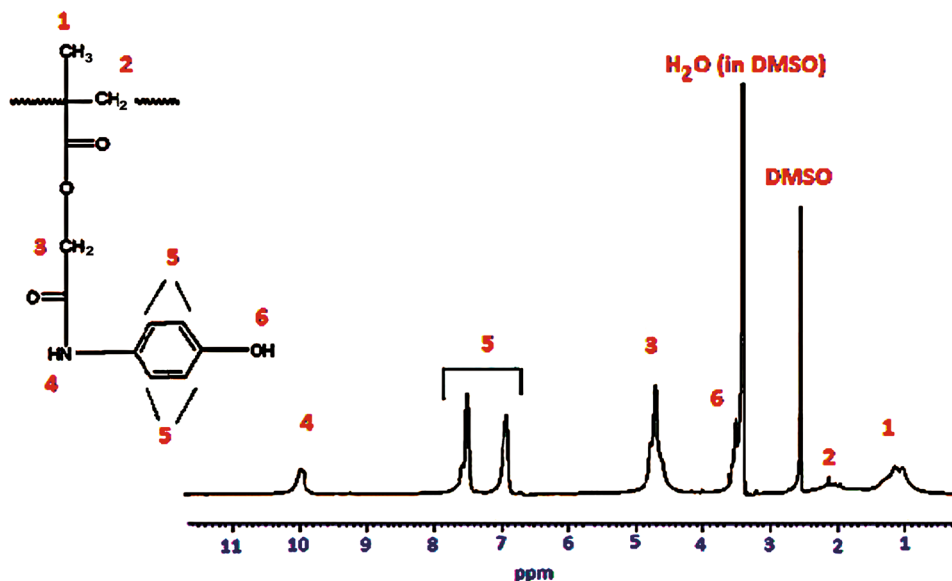
Fig. 1 The FTIR spectrum of poly(HAOEME)

Fig. 2 ^1H NMR spectra of poly(HAOEME)

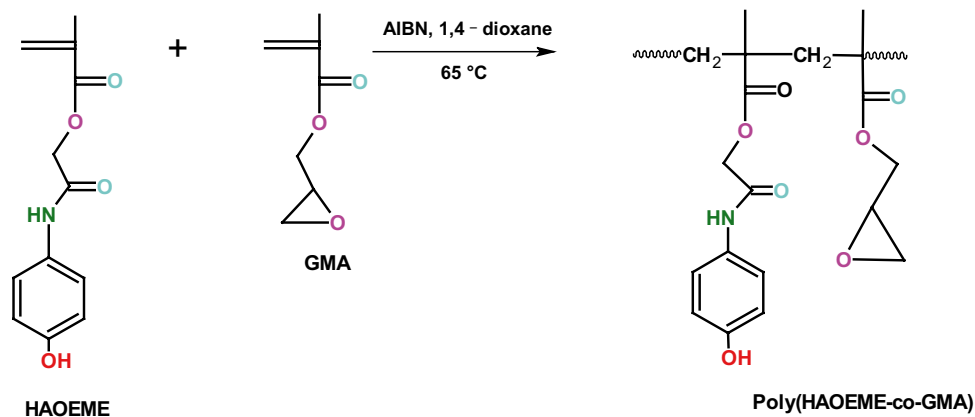


1640 cm^{-1} . The double bond peaks of the aromatic rings are observed at 1610 , 1508 , and 1480 cm^{-1} .

NMR spectrum

Figure 4 shows the ^1H and ^{13}C NMR spectrum of a copolymer sample and characteristic peaks in both spectra corresponding to the copolymer formula. It is consistent with the molecular structure in both sets of spectroscopic data. In the ^1H NMR spectrum, the peak seen at 10 ppm is attributed to the amide HN proton. The peaks at $6.8\text{--}7.8\text{ ppm}$ represent aromatic protons. Signals of the epoxide ring protons are observed at 2.4 and 3.3 ppm . The peak belonging to the proton in the OH group found in the HAOEME units is observed at 3.2 ppm . The characteristic peaks in the ^{13}H NMR spectrum are as follows: $166\text{--}169\text{ ppm}$ amide and ester carbonyl peaks, $115\text{--}155\text{ ppm}$ aromatic carbon peaks, 48 and 55 ppm epoxide ring carbons. The ^1H and ^{13}C NMR evaluations of the other unspecified groups are shown in Fig. 3.

Scheme 2 Synthesis of poly(HAOEME-co-GMA)



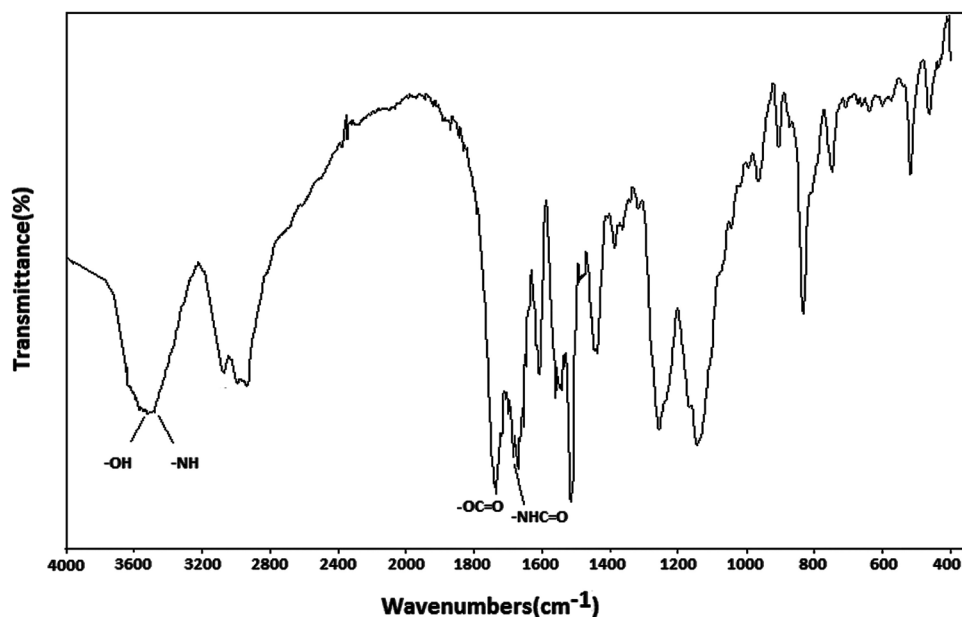
Copolymer compositions

By free radical solution polymerization, seven different ratios of HAOEME–GMA copolymers were prepared in the 1,4-dioxane solvent with AIBN as initiator. The composition of the copolymer was determined with the aid of elemental analysis (N content of HAOEME units). Table 1 shows the values obtained.

Molecular weights of polymers

Gel permeation chromatography was used to determine the molecular weights of the polymers using polystyrene as standard and tetrahydrofuran as solvent. Table 2 displays the M_w and M_n values and polydispersity index (M_w/M_n) of the polymers. The polydispersity index values of the polymers varied between 1.66 and 1.91 . The theoretical value of M_w/M_n is $1.5\text{--}2.0$, which means that the termination is radical and disproportionate. It is well known that the termination

Fig. 3 The FTIR spectrum of poly(HAOEME-co-GMA) (0.53:0.47)



results in disproportionality in the homopolymerization of GMA. When the poly(HAOEME) and poly(GMA) polydispersity indices were examined, the disproportionate chain

termination was higher than the combination. It is also clear that the M_w/M_n values in copolymerization depend on chain termination reactions in homopolymerization.

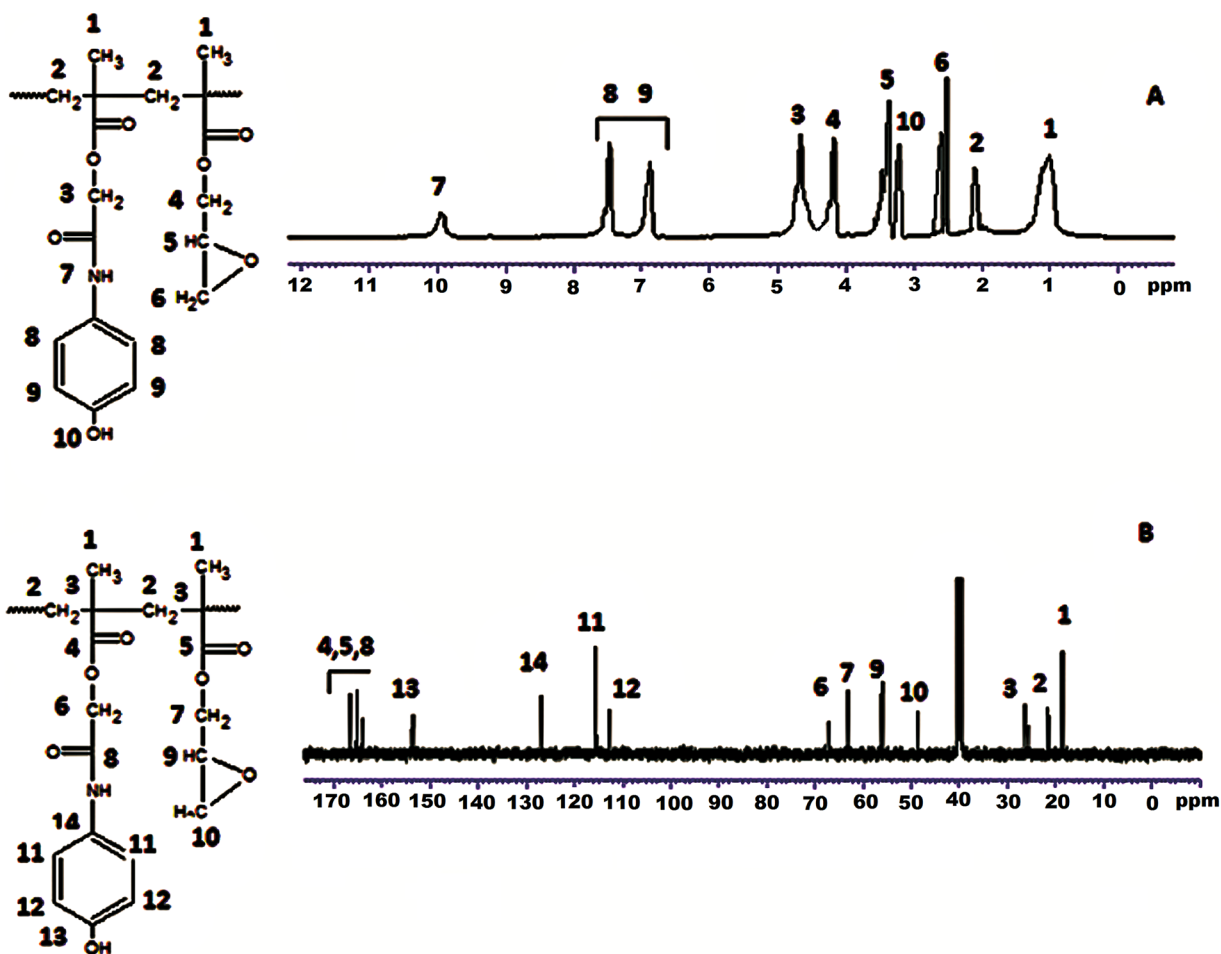


Fig. 4 (A), ^1H NMR and (B), ^{13}C NMR spectra of poly(HAOEME-co-GMA) (0.53:0.47)

Table 1 The monomer compositions in the feed and the copolymer

Sample	Feed composition (mol fraction)		Conv. (%)	N Content (%)	Copolymer composition (mol fraction)	
	HAOEME (M_1)	GMA (M_2)			HAOEME (m_1)	GMA (m_2)
1	0.20	0.80	8.50	2.78	0.34	0.66
2	0.30	0.70	9.50	3.54	0.46	0.54
3	0.40	0.60	9.90	3.77	0.51	0.49
4	0.50	0.50	8.90	3.89	0.53	0.47
5	0.60	0.40	9.25	4.12	0.57	0.43
6	0.70	0.30	9.50	4.53	0.66	0.34
7	0.80	0.20	9.80	4.95	0.74	0.26

Hydrogen bonding effects on the copolymerization

The functional groups (C=O, NH, OH) that HAOEME and GMA monomers had in the side branch were electron acceptors. N and O donor atoms in particular could form strong H bonds thanks to their unpaired electrons. In addition, these monomers were likely to interact between functional groups or via H bonds between macro radicals. This situation did not prevent HAOEME–GMA monomer pairs from providing sufficient activity in free radical copolymerization. This effect is displayed in Scheme 3.

The effect of hydrogen bonds on methacrylate-based polymers is manifested in applications such as surface coatings and self-healing adhesives [40, 41]. In addition, hydrogen bonds are present in many other functional groups and positively affect the molecule.

Monomer reactivity ratios

The r_1 and r_2 values of the HAOEME and GMA monomers were obtained by the F-R and K-T linearization method. Table 3 shows the parameters obtained with the F-R and K-T equations. Figure 5a, b shows the graphs drawn using the F-R and K-T parameters.

The values are presented as follows:

Table 2 Molecular weights and polydispersity index of polymers

Polymer	m_1^a	$\overline{M}_w \times 10^4$	$\overline{M}_n \times 10^4$	$\overline{M}_w/\overline{M}_n$
Poly(HAOEME)	1.00	5.25	2.90	1.81
Poly(HAOEME-co-GMA)	0.34	4.59	2.76	1.66
	0.46	4.82	2.82	1.71
	0.51	4.88	2.77	1.76
	0.53	5.19	2.86	1.81
	0.57	5.38	2.92	1.84
	0.66	5.67	3.00	1.89
	0.74	6.80	3.56	1.91
Poly(GMA)	0.00	4.61	2.36	1.95

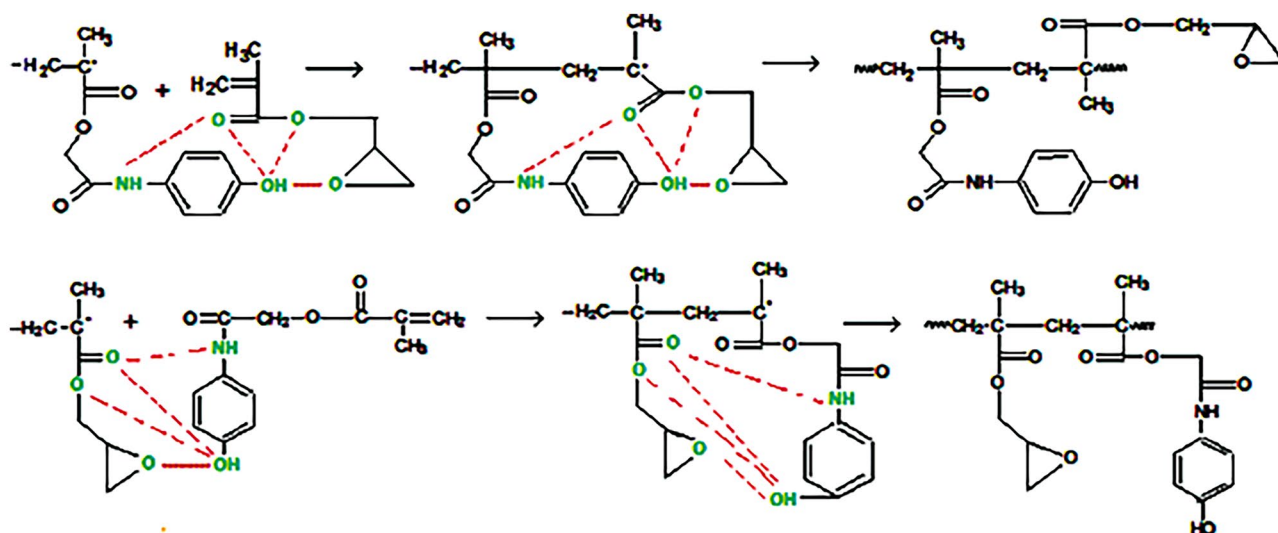
^a m_1 is the mole fraction of HAOEME in the copolymer.

Methods	r_1	r_2	$r_1 r_2$	$1/r_1$	$1/r_2$
F-R	0.50	0.29	0.15	2.00	3.45
K-T	0.50	0.25	0.13	2.00	4.00
Average	0.50	0.27	0.14	2.00	3.73

The r_1 and r_2 values calculated by the F-R and K-T methods were less than 1. The r_{HAOEME} value was greater than the r_{GMA} value. This indicates that HAOEME had higher reactivity than GMA. HAOEMA was more involved in the copolymer due to the hydrogen bonds likely to occur between the OH and NH groups in the copolymeric HAOEME units. The calculated $r_1 r_2$ value close to zero means that this type of copolymer has an alternative tendency. In the HAOEMA–GMA system, monomers that are the active centers always tend to add other types of monomers. The monomers are neatly arranged in the polymer chain. The entry of monomer molecules into the copolymer chain does not depend on the starting composition. The monomers are neatly lined up in the copolymer. The reason why HAOEMA was more active can be explained by the constitution of the H bond between OH groups and the carbonyl groups shown in Scheme 3. Therefore, it can be said that the formation of the copolymer proceeds by adding mainly GMA comonomers to the HAOEME macroradical. However, the same situation was not observed in radical copolymerization between other methacrylate monomers [42] due to the lack of H bond between monomeric structures. In such copolymeric systems, alternating copolymers containing predominantly methacrylate monomers are formed [43]. The H bond effect in the poly(HAOEMA-co-GMA) system was the most effective parameter in determining copolymer type.

Glass transition temperatures

The glass transition temperatures of the copolymers were determined with DSC. DSC thermograms of samples were recorded at a heating rate of 10 °C/min by heating up to 250 °C in N_2 atmosphere. The midpoint of the process zone in the DSC thermograms was accepted as the T_g . Endothermic



Scheme 3 Hydrogen bonding effects on copolymerization

transition was observed in DSC thermograms of all polymers. A single T_g value was determined from DSC thermograms of all copolymers. This is the most important proof that copolymeric structures are not a mixture of homopolymers. Figure 6 shows DSC curves for some copolymers. The T_g value of poly(GMA) was 74 °C, and poly(HAOEME) was 119 °C. The high T_g value of poly(HAOEME) was due to the strong H bonds between HAOEME units. The H bond causes the free volume of the poly(HAOEME) to decrease and the T_g value to increase. Hydrogen bonds decrease the polymer molecule mobility. One of the main properties of the polymer with side chain hydroxyl groups is the hydrogen bonding between the ester and hydroxyl groups on adjacent chains, and the inter-chain interaction resulting from dipole-dipole interactions [44]. This is an important result of the hydroxyl group in the side branch of poly(HAOEME).

Table 4 reveals that the T_g values of the copolymers are among those of the homopolymer. The thermal properties of copolymers are closely related to the microstructure of the copolymeric structure. The elasticity of the polymer chains and the value of the intermolecular interaction energy significantly affect the T_g value. All structural features that reduce

intermolecular flexibility, such as H bonds, cause an increase in the T_g value. When the poly(HAOEME-co-GMA) system was examined, it was clear that the T_g value increased with an increase in the HAOEME units in the copolymeric structure. This was due to the strong H bonds between HAOEME units. H bonds decreased the flexibility of copolymer molecules and caused an increase in T_g values.

According to the theory of Gibbs and Di Marzio, the glass transition process of a polymer is considered in terms of the thermodynamic state of the system determined by the number of possible conformations of the macromolecule. In this theory, the glass transition is regarded as a second-order phase transition.

The Gibbs–Di Marzio equation is given below. [45]:

$$T_g = \Phi_{\text{HAOEME}} T_{g\text{HAOEME}} + \Phi_{\text{GMA}} T_{g\text{GMA}} \quad (4)$$

where Φ is the mole fraction of the monomers in the composition and T_g is the glass transition temperature of the respective homopolymer.

Another relationship showing the effect of the composition on T_g in copolymers was proposed by Fox [46], as shown in the equation below:

Table 3 F-R and K-T parameters for poly(HAOEME-co-GMA) systems

Sample	F	f	G	H	η	ϵ
1	0.250	0.515	-0.235	0.121	-0.409	0.211
2	0.429	0.852	-0.075	0.216	-0.111	0.322
3	0.667	1.041	0.026	0.427	0.023	0.485
4	1.000	1.128	0.113	0.887	0.084	0.662
5	1.500	1.326	0.368	1.697	0.171	0.789
6	2.333	1.941	1.131	2.805	0.403	0.861
7	4.000	2.846	2.595	5.622	0.461	0.925

$$\alpha = (H_{\text{max}} - H_{\text{min}})^{1/2} = 0.454.$$

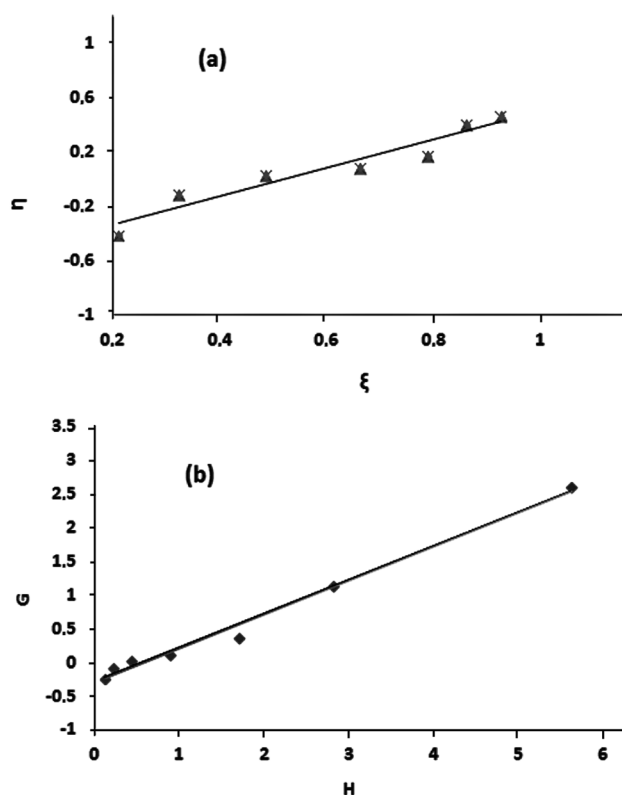


Fig. 5 (a), F-R plots and (b), K-T plots for determining the monomer reactivity ratios in the copolymerization of poly(HAOEME-co-GMA)

$$\frac{1}{T_g} = \frac{W_{\text{HAOEME}}}{T_{g\text{HAOEME}}} + \frac{W_{\text{GMA}}}{T_{g\text{GMA}}} \quad (5)$$

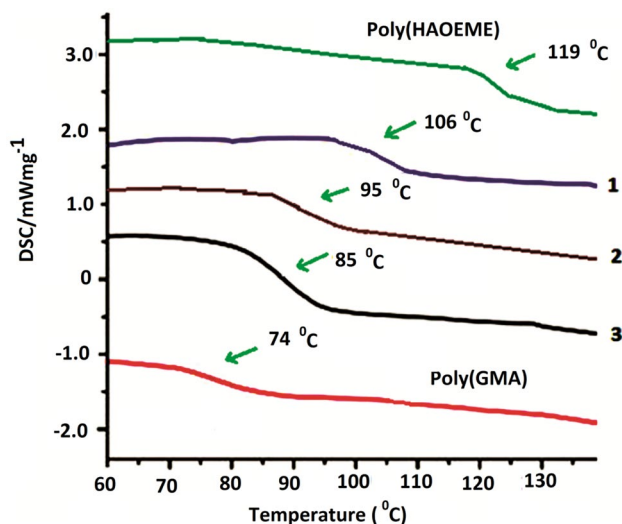


Fig. 6 Variation of T_g (°C) with composition of poly(HAOEME-co-GMA) system. 1 (66% HAOEME by mole in copolymer), 2 (53% HAOEME by mole in copolymer), 3 (46% HAOEME by mole in copolymer)

Table 4 Comparison of observed T_g value of copolymers with calculated T_g value from Fox and Gibbs–Di Marzio equations

Sample	W_1^a	W_2^b	$T_g(^{\circ}\text{C})^c$	$T_g(^{\circ}\text{C})^d$	$T_g(^{\circ}\text{C})^e$
GMA	0	100	-	-	74
1	0.34	0.66	85	89	79
2	0.46	0.54	89	94	85
3	0.51	0.49	92	97	91
4	0.53	0.47	92	98	95
5	0.57	0.43	94	99	100
6	0.66	0.34	99	104	106
7	0.74	0.26	103	107	113
HAOEME	100	0	-	-	119

^aWeight fraction of HAOEME in the copolymer.

^bWeight fraction of GMA in the copolymer.

^cCalculated by Fox equation.

^dCalculated by Gibbs–Di Marzio equation.

^eObserved in relating DSC curve.

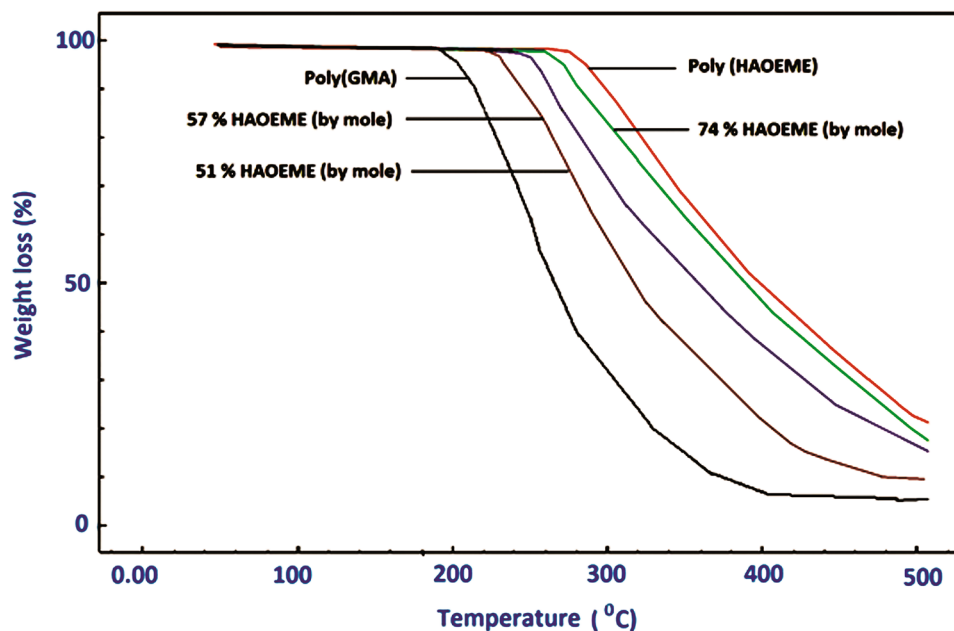
where W is the weight fractions of related monomers in the copolymer. Table 4 shows the T_g values obtained from the Gibbs–Di Marzio and Fox equations.

Positive deviations were observed in the T_g values obtained by both methods. These methods do not consider parameters such as free volume, steric effect, copolymer type, or thermodynamic and energetic interactions that affect the glass transition temperature. Therefore, the values obtained by both methods showed positive deviations from the T_g values obtained by DSC.

Thermogravimetric analysis

Figure 7 shows TGA curves for poly(HAOEME), poly(GMA), and three copolymers. The initial decomposition temperature values (IDT) of poly(HAOEME) and poly(GMA) were determined as 285 and 184 °C, respectively. Thermal degradation of poly(HAOEME) occurred in one step. The thermal resistance of this polymer is higher than poly(GMA). The high thermal resistance of poly(HAOEME) is because of the strong H bonds between the NH and OH groups in its structure. It is known that polymers with similar structures have high thermal stability [47]. Thermal degradation of poly(GMA) took place in two steps. In the first step, the depolymerization process began at the unsaturated chain ends, followed by random chain breakage at higher temperatures. The residual % left by poly(HAOEME) and poly(GMA) at 450 °C was 39 and 2, respectively. For HAOEME–GMA copolymers, the residual amount at 450 °C was increased with increasing HAOEME units in the copolymer.

Fig. 7 TGA curves for homopolymers and some copolymers



According to the TGA data, it was observed that the thermal stability of the copolymers was between 190 and 275 °C depending on the composition. Table 5 gives a comparison of some thermogravimetric data of copolymer and homopolymers.

The thermal resistance of the copolymers was between the stability of the homopolymer that formed them. It was observed that the thermal resistance of copolymers increased with an increase in the number of HAOEME units in the copolymeric structure. The thermal degradation behavior of homopolymers and copolymers is parallel to that of like methacrylate derivatives mentioned in the literature [48].

In this context, it is necessary to draw attention to the thermal degradation behavior of poly(methacrylate) carrying different functional groups in the side chain. Some polymethacrylates break down relatively easily into their monomer by the effect of heating. On the other hand, in some polymers, ester decomposition occurs without depolymerization. In some methacrylate polymers, thermal degradation takes place in the form of breakage in the main chain, which is called depolymerization, and degradation continues with ester decomposition at high temperatures; the elimination of small molecules and the cyclic anhydride structure occurs as the temperature rises further [49].

Decomposition kinetics

The Ozawa and Kissinger integral methods, which are independent of the reaction order, are widely used in calculating the thermal degradation activation energy value of polymers. The decrease in the mass of the polymers due to the programmatically increased or decreased temperature in the TG

method can be examined as a function of temperature or time. The activation energy (E_a) values can be calculated using the data obtained from TG. Commonly used methods have been developed for this purpose.

TG curves were obtained at various heating rates of synthesized polymers, and the E_a value of polymers was calculated using Ozawa methods. Thermograms of all-polymer samples were obtained at five different heating rates (5.0, 10.0, 20.0, 30.0 and 40.0 °C min⁻¹) in an inert N₂ atmosphere. While obtaining the thermograms, a positive change was observed in the upper temperatures of the curves with an increase in the heating rate. At high rates, an increase in peak temperatures occurs because of the shorter time the polymeric material is exposed to the decomposition temperature. At higher rates, a heat mismatch occurs between the outer surface and the interior of the deformed polymer. Since the outer surface of the polymer becomes hotter than the inner section, fragmentation

Table 5 Some TGA results of the copolymers

Polymer	IDT ^a	Temperature (°C)			Residue (%) at 450 °C
		10	35	50	
Poly(HAOEME)	282	301	361	398	28
Poly(GMA)	184	205	233	246	2
Poly(HAOEME-co-GMA)					
(51/49)	222	247	298	320	12
(57/43)	248	280	320	360	28
(74/36)	270	281	340	390	35

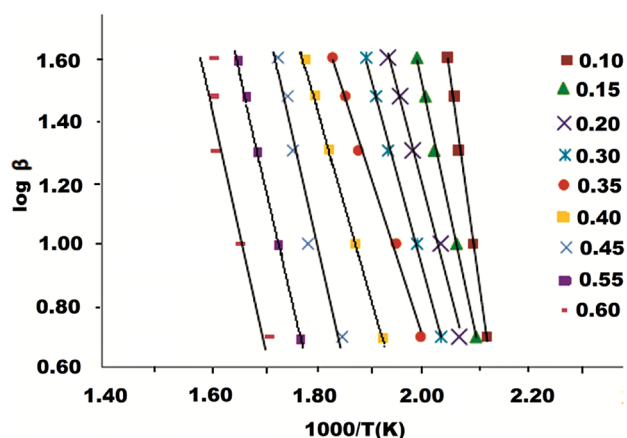


Fig. 8 Ozawa plots of the logarithm of the heating rate ($\log \beta$) versus the reciprocal of the temperature ($1/T$) at different conversions for poly(HAOEME-co-GMA) (0.53:0.47)

occurs on the outer surface at higher temperatures due to the increase in the heating rate.

The E_a of the obtained polymers was determined according to the equation of Ozawa [50]:

$$E_d = -\frac{R}{b} \left[\frac{d \log \beta}{d(1/T)} \right] \quad (6)$$

where R is the gas constant, b is the constant (0.4567), and β is the heating rate.

The Ozawa method is an excellent isothermal method that does not consider the degree of reaction. When the results of the Ozawa analysis for poly(HAOEME-co-GMA) (34:66) were plotted, the data consisting of parallel lines confirming the accuracy of the method used were as those in Fig. 8. The average E_a value of poly(HAOEME) was calculated as around 150 kJ/mol. The E_a values of the copolymers showed a random distribution independent of the copolymer composition. The calculated E_a values of the polymers at different transformations can also be seen in Table 6.

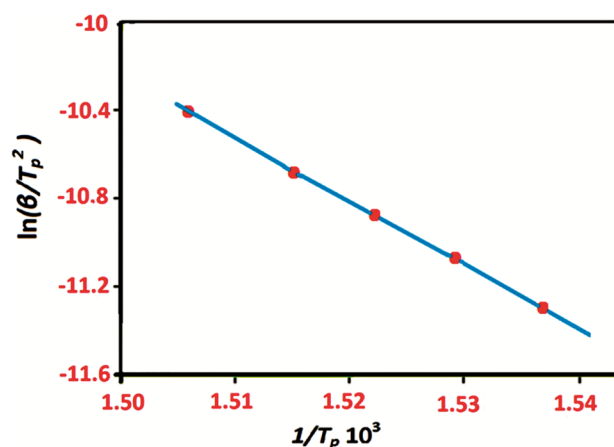


Fig. 9 For first degradation steps, Kissinger plot of poly(HAOEME-co-GMA) (0.53:0.47)

The Kissinger method is another method used to calculate the E_a values of polymers regardless of the reaction order [51]. The thermal decomposition activation energy of the prepared polymer samples was also calculated using the Kissinger method:

$$\frac{d(\ln(\beta/T_p^2))}{d(1/T_p)} = \frac{E_a}{R} \quad (7)$$

where β is the heating rate, T_p is the maximum temperature, and R is the ideal gas constant. From a plot of $\ln(\beta/T_p^2)$ versus $1/T_p$ and fitting to a straight line, the activation energy E_a can be calculated from the slope. Figure 9 shows the Kissinger plot of the first degradation stage of the poly(HAOEME-co-GMA) (0.53:0.47) copolymer sample. The thermal degradation activation energy values of the polymers in two different temperature ranges were calculated by Kissinger method.

The E_a values calculated for poly(HAOEME) are 175.23 and 181.38 kJ/mol for the first and second degradation steps,

Table 6 Evident activation energy of examined thermal degradation copolymers in N_2

Sample	10	15	20	30	35	45	50	55	60
Poly(HAOEME)	131.93	149.44	152.23	147.71	157.50	168.54	169.33	155.53	144.60
Poly(HAOEME 34%-GMA)	98.45	126.46	146.21	145.40	132.93	125.80	125.30	128.18	154.14
Poly(HAOEME 46%-co-GMA)	129.18	136.10	138.22	129.18	132.36	135.22	133.31	131.42	138.12
Poly(HAOEME 51%-co-GMA)	135.45	139.69	139.19	127.74	134.47	127.29	129.16	126.60	165.80
Poly(HAOEME 53%-co-GMA)	139.27	145.76	137.36	141.53	135.19	126.74	143.56	138.25	171.96
Poly(HAOEME 57%-co-GMA)	139.91	148.58	133.93	136.97	144.53	168.80	135.41	155.27	143.47
Poly(HAOEME 66%-co-GMA)	135.80	113.53	150.86	149.80	159.87	147.58	165.39	171.38	177.37
Poly(HAOEME 74%-co-GMA)	133.14	110.40	143.12	131.21	165.10	125.49	155.32	143.54	168.62

Table 7 Regression coefficients and degradation apparent activation energies (E_a) by Kissinger equation for copolymers and HAOEME and GMA homopolymers

Polymer	First stage		Second stage		R
	TG range(°C)	E_a (kJ/mol)	TG range(°C)	E_a (kJ/mol)	
Poly(HAOEME)	290–350	175.23	350–445	181.38	0.98
Poly(GMA)	195–345	117.2	340–450	169.33	0.99
Poly(HAOEME 34%-co-GMA)	235–345	138.66	345–450	119.48	0.99
Poly(HAOEME 46%-co-GMA)	240–350	143.39	340–445	138.24	0.98
Poly(HAOEME 51%-co-GMA)	250–355	151.60	340–450	148.86	0.98
Poly(HAOEME 53%-co-GMA)	260–350	159.43	340–445	185.20	0.99
Poly(HAOEME 57%-co-GMA)	270–345	157.98	345–440	177.82	0.99
Poly(HAOEME 66%-co-GMA)	275–355	155.20	345–445	147.17	0.98
Poly(HAOEME 74%-co-GMA)	280–345	145.53	345–450	189.94	0.99

respectively. The same values are 117.2 and 169.33 kJ/mol for poly(GMA). The E_a values of the copolymers were also determined at two different decomposition temperatures. The first temperature range was 235–345 °C, and the average E_a value for this range was 150.2 kJ / mol. The second temperature range was 255–450 °C and the average activation energy for this range was found to be 158.1 kJ / mol. The E_a values obtained showed a random distribution independent of the copolymer composition. The probable reason for this may be the different distribution of monomers in the microstructure of the copolymers. In particular, 53% and 74% HAOEME copolymers have higher E_a values for the second degradation step than poly(HAOEME). Table 7 presents E_a values of polymers obtained from the Kissinger method [52].

Antimicrobial screening

All polymers showed moderate activity similar to standard drugs. The average of three experiments was calculated and is displayed in the data listed in Tables 8 and 9.

The results show that biological activity increases with increasing polymer concentration. The findings show that the polymers analyzed have mild biological activity similar to conventional drugs such as penicillin and teicoplanin. The biological activity of poly(HAOEME) was better than that of copolymers. A possible reason for this is the phenolic hydroxyl groups carried by the polymer. The hydroxyl group of poly(HAOEME) was shown to be important for its effect on membrane properties and probably for its antimicrobial activity. These results are related to the O-H bond dissociation energy of the phenolic hydroxyl group in poly(HAOEME) and the proton affinity involved in the electron donating ability. To sum up, phenolic hydroxyl and amide / ester groups significantly increase the biological activity of the molecule in which they are located. In addition, phenolic hydroxyls are electron-donating groups and contribute to the biological activity of the molecules [53, 54].

As expected, the activity of the copolymers against microorganisms increased with the increase in the HAOEME

Table 8 Antimicrobial effects of the compounds (mm of zones)

Compounds	<i>Pseudomonas aeruginosa</i>	<i>Escherichia coli</i>	<i>Proteus vulgaris</i>	<i>Salmonella enteritidis</i>	<i>Klebsiella pneumoniae</i>	<i>Staphylococcus aureus</i>	<i>Candida albicans</i>
Poly(HAOEME)	11±1	10±0.5	11±1	10±2	-	11±0.5	10±1
Poly(HAOEME-co-GMA)							
34 / 66	6±1	5±0.5	5±0.5	-	6±0.75	6±1	7±0.5
46 / 54	7±1	6±0.25	7±	5±0.5	7±0.75	7±0.75	-
51 / 49	9±1	7±0.75	8±0.5	6±1	-	-	8±1.5
53 / 47	10±0.75	8±1	-	-	9±0.5	9±0.25	10±1
57 / 43	11±0.25	-	-	7±0.5	10±2	10±0.25	-
66 / 34	13±1	9±0.25	8±0.25	9±1	-	-	11±0.5
74 / 26	14±0.75	10±1	8±0.5	-	12±1	11±0.5	-
Penicillin G	16±0.5	12±0.5	9±0.25	16±1	18±1	17±1	35±0.75
Teicoplanin	18±1	18±2	11±1	22±2	25±2	12±1	15±1
DMSO	-	-	-	-	-	-	-

Compound concentration: 50 µg/disc; the symbol (-) indicates that the compounds do not have any activity against the microorganisms. DMSO: dimethyl sulfoxide (control). Results calculated are means ± SD, superscript means are statistically significance at $p < 0.05$.

Table 9 Antimicrobial effects of the compounds (mm of zones)

Compounds	<i>Pseudomonas aeruginosa</i>	<i>Escherichia coli</i>	<i>Proteus vulgaris</i>	<i>Salmonella enteritidis</i>	<i>Klebsiella pneumoniae</i>	<i>Staphylococcus aureus</i>	<i>Candida albicans</i>
Poly(HAOEME)	14±2	12±1	13±1	12±0.5	13±1	14±1.5	12±1
Poly(HAOEME-co-GMA)							
34 / 66	8±0.5	6±1	7±0.75	-	9±1	9±0.5	9±1
46 / 54	10±2	7±1	8±0.5	7±0.5	10±1	10±1	-
51 / 49	11±1	7±0.25	9±1	8±2	-	-	10±1
53 / 47	13±1.5	8±0.5	-	-	11±0.5	11±1	11±1
57 / 43	14±2	-	-	9±1	12±0.5	12±0.75	-
66 / 34	15±0.75	9±1	10±0.5	10±0.25	13±1	-	12±1.5
74 / 26	15±2	11±1	11±0.5	-	14±1	13±0.25	14±2
Penicillin G	16±1.5	12±1	9±0.5	16±2	18±1	17±2	35±2
Teicoplanin	18±1	18±2	11±1.5	22±1	25±1	12±2	15±1.5
DMSO	-	-	-	-	-	-	-

Compound concentration: 100 µg/disc; the symbol (-) indicates that the compounds do not have any activity against the microorganisms. DMSO: dimethyl sulfoxide (control). Results calculated are means ± SD, superscripts indicate statistical significance at $p < 0.05$.

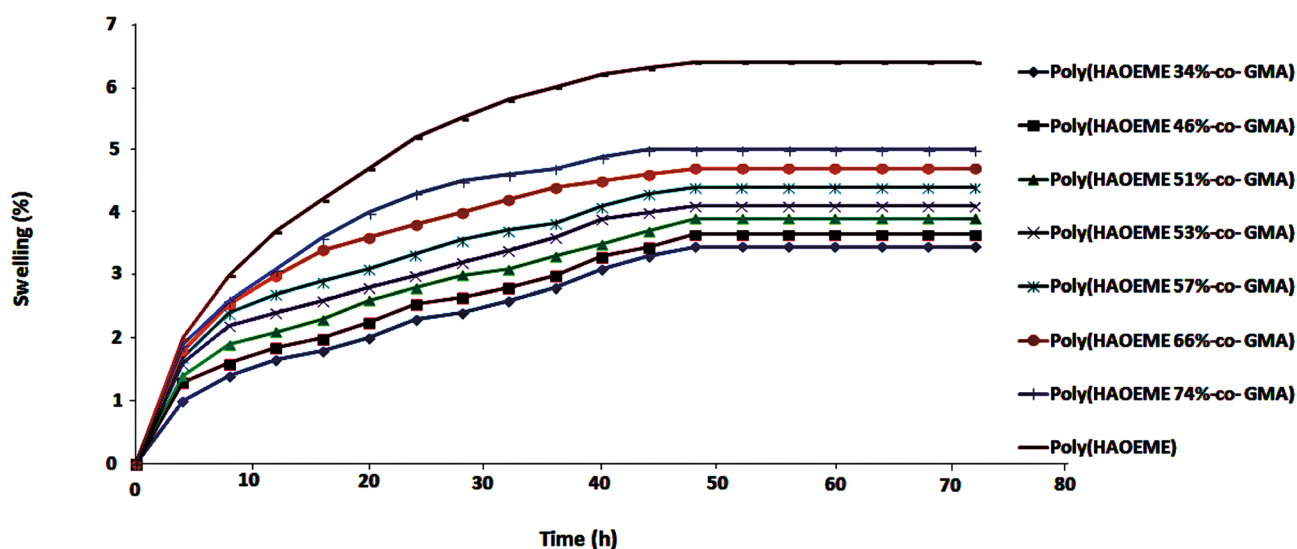
content of the copolymers. The obtained values indicate that poly(HAOEME) and certain copolymers have strong biological activity in *Pseudomonas aeruginosa* bacteria..

Pseudomonas is an important bacteria genus that is widely found in the environment and in soil and water. *Pseudomonas aeruginosa* can cause infections in the blood, lungs (pneumonia), or other parts of the body after surgery.

Tables 8 and 9 reveal that the biological activity of the copolymers is lower than that of the drugs. It can be said that the antibacterial and antifungal effect of the synthesized copolymers was due to functional groups such as phenolic hydroxyl, ester, and amide in HAOEME and GMA units. The donor systems such as OH, NH, and C=O in the

copolymer structure might have inhibited the enzyme development, because enzymes looking for a free hydroxyl group tend to be extremely sensitive to deactivation by copolymers. The results obtained are consistent with the literature [55].

The results show that HAOEME-GMA copolymers can be used as biomaterials. These copolymers can be used in paints on hospital room walls and everyday objects such as doorknobs, children's toys, computer keyboards, and telephones. The antimicrobial properties of a polymer play an important role in many of its applications. Contamination by microorganisms is of great concern in fields such as medical devices, health care products, water purification systems, and hospital and dental equipment. One possible

**Fig. 10** Variation of S% values with time at 37 °C at pH 7

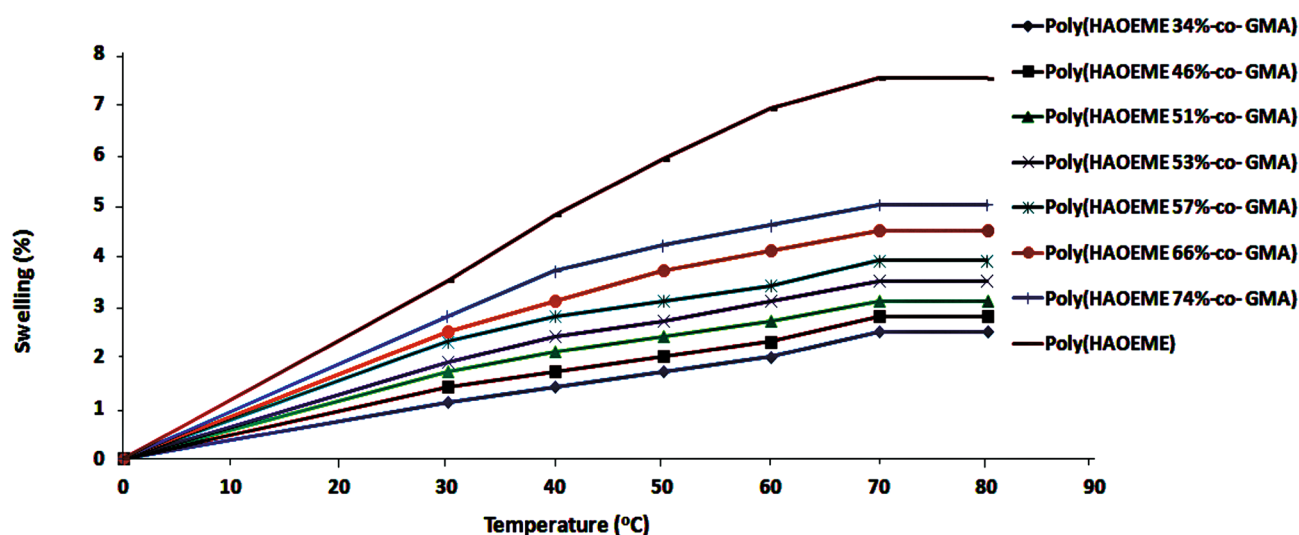


Fig. 11 Variation of S% values with temperature for 24 h at pH 7

way to avoid microbial contamination is to develop materials possessing antimicrobial properties.

Swelling behavior of the polymers

Figure 10 shows the change of average % swelling values of polymers over time. As seen in Fig. 10, the % swelling value of all polymers over time increased and reached equilibrium at around 43 h. The highest swelling value belonged to poly(HAOEME), and this value varied between 2.0 and 6.4% from the initial measurement to the last measurement. With the rise of HAOEME amounts in the copolymer structure, the swelling rate of copolymers increased. While the swelling values of the copolymer sample containing 34% HAOEME are between 1 and 3.45, this value was between 1.9 and 5 for the copolymer containing 74% HAOEME. It was observed that the % swelling values of all polymers reached equilibrium after about 50 h. Thanks to the hydroxyl group HAOEME units carry, the hydrophilic character of the copolymers is becoming dominant. Thus, more water molecules can enter the copolymeric structure via H bonds. Over time, the adherence of water molecules increased and then reached equilibrium.

Figure 11 shows the results of temperature change of average % swelling values of polymers, and it can be inferred from the figure that swelling values for all polymers can be changed with temperature. All polymers first increased with the increase in temperature, then reached equilibrium around 70 °C. The highest % swelling value belonged to poly(HAOEME), and this value was 7.5 at 70 °C. The swelling values of other polymers were similar to the data presented in Fig. 10. All polymers showed a rapid

swelling behavior between 40 and 70 °C. This situation increased the temperature of the polymer molecules, which can be attributed to their increased mobility [56]. Also, the possibility of H bonds forming between HAOEME and GMA units in the copolymer can be explained as follows. The swelling percentage increases as a result of breaking of possible H bonds between the HAOEME and GMA units in copolymers with rising temperature. Similar results can be found in the literature [57, 58]. As the amount of GMA increased in the copolymer, the swelling values against temperature remained lower. In general, a significant increase in swelling values of copolymers was observed with the rise in temperature.

Conclusion

A new HAOEME monomer was synthesized containing a phenolic hydroxyl group in the side branch. The new monomer and homopolymer were characterized using spectroscopic methods. Then, copolymers of HAOEME monomer and commercial GMA monomer were synthesized by free radical polymerization method at seven different feed rates. The structural characterization of the copolymers obtained was carried out using FTIR and NMR techniques.

The composition of the poly(HAOEME-co-GMA) system was calculated by the amount of N in HAOEME units. r_1 and r_2 values of HAOEME-GMA system were calculated using the F-R and K-T linear graphic methods. The reactivity ratios of the copolymers were determined by the F-R and K-T methods. The average r value of poly(HAOEME) was 0.5, and for poly(GMA) was 0.27. The $r_1.r_2$ value of this system was 0.14. It was concluded that the HAOEME

monomer is more reactive, so the copolymers are rich in HAOEME. Looking at the $1/r_1$ value of the GMA monomer, it is seen that it tends to add more other monomers. The fact that the $r_1.r_2$ value is close to zero indicates that this type of copolymerization is optional. Poly(HAOEME) and poly(GMA) monomers are alternately arranged along the chain, and an alternating copolymer is obtained. The reason why poly(HAOEME) is more involved in the copolymer is the strong H bonds formed by the OH groups it carries. The T_g value of poly(GMA) was 74 °C, and poly(HAOEME) was 119 °C. It was observed that the T_g values of the copolymers were between the T_g values of the homopolymers and were between 113 and 119 °C. In addition, the theoretical T_g values were calculated using the Fox and Gibbs–Di Marzio equations, and it was determined that they were compatible with the real T_g . The initial decomposition temperature values (IDT) of poly(HAOEME) and poly(GMA) were determined as 285 and 184 °C. It was seen from TGA curves that poly(HAOEME) was more stable than poly(GMA). The reason for this is the hydrogen bonds formed by the OH groups carried by the HAOEME units. It was also observed that the thermal stability of the copolymers increased as the HAOEME content in the copolymer increased. From the non-isothermal degradation data, the kinetic parameters such as E_a for the polymer have been calculated using Ozawa and Kissinger methods. From the Kissinger method, the first temperature range was 195–345 °C, and the average E_a value for this range was 150.2 kJ/mol, and the second temperature range was 340–450 °C, and the average activation energy for this range was found to be 158.1 kJ/mol. Similar results were obtained with the Ozawa method. There is a good correlation between the calculated values for activation energy between methods, and there is a similar change trend of E_a between the two methods. The polydispersity index determined by GPC was around 2, indicating that the termination reactions in this system are disproportionate. The antimicrobial effects of poly(HAOEMA) and copolymers on various microorganisms were investigated in DMSO solution at two different concentrations (50 and 100 µg). Biological activity increased with increasing sample concentration. According to the biological activity tests performed, the copolymer has strong activity on the *Pseudomonas aeruginosa* microorganism. The water absorption capacity of the copolymers was investigated by swelling experiments. The highest swelling value belonged to poly(HAOEME), and this value varied between 2.0 and 6.4% from the initial measurement to the last measurement. With temperature and time, the swelling capacity of the polymers increased and stabilized after a certain value. With increasing HAOEME units in the copolymer, the % swelling values of polymers increase. This is probably because of the hydrophilic OH groups they carry.

Acknowledgements This study is supported by Afyon Kocatepe University Scientific Research Projects Coordination Unit. Project Number 14-FENB-26. The author is grateful to Dr. Zeki GÜRLER for the study of biological behavior.

References

1. Cironi A, Alvarez M, Albericio F (2006) Solid-phase chemistry in the total synthesis of non-peptidic natural products. *Mini Rev Med Chem* 6:11–25
2. Yakuphanoglu F, Erol I (2004) A novel organic semiconducting material: 2-(3-mesityl-3-methylcyclobutyl)-2-keto-ethyl methacrylate (MCKEMA). *Physica B: Condensed Matter* 352:378–382
3. Duncan R (2003) The dawning era of polymer therapeutics. *Nat Rev Drug Discov* 2:347–360
4. Erol I, Soykan C, Ahmedzade M (2002) Monomer reactivity ratios of the 2-(3-mesityl-3-methylcyclobutyl)-2-hydroxyethyl methacrylate and styrene system from $^1\text{H-NMR}$. *J Polym Sci Part A-Polym Chem* 40:1756–1763
5. Demirelli K, Coskun M, Erol I (2000) Copolymerization and monomer reactivity ratios of 2-(3-mesityl-3-methylcyclobutyl)-2-hydroxyethyl methacrylate with acrylonitrile. *Eur Polym J* 36:83–88
6. Erol I, Sarkaya S (2012) Copolymers of methacrylic and styrenic monomer based on the naphthalene: Synthesis, characterization, monomer reactivity ratios, and thermal properties. *J Polym Res* 19:9957
7. Soykan C, Erol I (2003) Synthesis, spectral, and thermal properties of homo- and copolymers of 2-[(5-methylisoxazol-3-yl) amino]-2-oxo-ethyl methacrylate with styrene and methyl methacrylate and determination of monomer reactivity ratios. *Eur Polym J* 39:2261–2270
8. Kenawya E-R, IAbdel-Hay F, REI-Shanshoury A.E.-R., HEL-Newehy M, (1998) Biologically active polymers: synthesis and antimicrobial activity of modified glycidylmethacrylate polymers having a quaternary ammonium and phosphonium groups. *J Control Release* 50:145–152
9. Lang M, Jianzhong B, Wang S (1999) Synthesis and characterization of polycaprolactone / poly(ethylene oxide) / polylactide tri-component copolymers. *J Biomater Sci Polym Ed* 10:501–512
10. Martin C, Aibani N, Callan JF, Callan B (2015) Recent advances in amphiphilic polymers for simultaneous delivery of hydrophobic and hydrophilic drugs. *Ther Deliv* 7:15–31
11. Wang H, Chen QW, Zhou SQ (2018) Carbon-based hybrid nanogels: a synergistic nanoplatform for combined biosensing, bioimaging, and responsive drug delivery. *Chem Soc Rev* 47:4198–4232
12. Bıcak TC, Soylemez S, Buber E, Toppare L, Yagci Y (2017) Poly(*o*-aminophenol) prepared by Cu(II) catalyzed air oxidation and its use a biosensing architecture. *Polym Chem* 8:3881–3888
13. Shi P, Zhang X, Liu Y, Duan Y, Li Y, Li Z, Han T (2020) A multi-stimuli-responsive AIE material switching among three emission states. *Mater Lett* 263:127214
14. Riess G (2003) Micellization of block copolymers. *Prog Polym Sci* 28:1107–1112
15. Moller S, Weisser J, Bischoff S, Schnabelrauch M (2007) Dextran and hyaluronan methacrylate based hydrogels as matrices for soft tissue reconstruction. *Biomol Eng* 24:496–504
16. Aydogdu Y, Erol I, Yakuphanoglu F et al (2003) Electrical conductivity and optical properties of copolymers based on 4-vinylpyridine and tetralincyclobutylhydroxyethylmethacrylate. *Synth Met* 139:327–334
17. Bhola R, Bhola SM, Liang H, Mishra B (2010) BBiocompatible denture polymers-a review. *Trends Biomater Artif Organs* 23:129–136

18. Hus S, Kolar M, Krajnc P (2016) Separation of heavy metals from water by functionalized glycidyl methacrylate poly (high internal phase emulsions). *J Chromatogr A* 1437:168–175
19. Reis AV, Fajardo AR, Schuquel ITA, Guilherme MR, Vidotti GJ, Rubira AF, Muniz EC (2009) Reaction of glycidyl methacrylate at the hydroxyl and carboxylic groups of poly(vinyl alcohol) and poly(acrylic acid): is this reaction mechanism still unclear? *J Org Chem* 74:3750–3757
20. Nasirtabrizi MH, Khodabandlou S, Zargin L, Parchehbaf Jadid A (2014) Modification of copolymers using nucleophilic reactions between glycidyl methacrylate and 9- anthracene carboxylic acid. *Int J Ind Chem* 5:6
21. Majer J, Krajnc P (2010) Amine functionalisations of glycidyl methacrylate based PolyHIPE monoliths. *Macromol Symp* 296:5–10
22. Ghosh S, Krishnamurti N (2000) Use of glycidyl methacrylate monomers for developing cross-linkable pressure sensitive adhesives. *Eur Polym J* 36:2125–2131
23. Yuan H, Yu B, Fan LH, Wang M, Zhu Y, Ding X, Xu F-J (2016) Multiple types of hydroxyl-rich cationic derivatives of PGMA for broad-spectrum antibacterial and antifouling coatings. *Polym Chem* 7:5709–5718
24. Guilherme MR, Reis AV, Takahashi SH, Rubira AF, Feitosa JPA, Muniz EC (2005) Synthesis of a novel superabsorbent hydrogel by copolymerization of acrylamide and cashew gum modified with glycidyl methacrylate. *Carbohydr Chem* 61:464–471
25. Jlassi K, Chandran S, Mi^ˆcu^ˆsik M, Benna-Zayani M, Yagci Y, Thomas S, Chehimi MM (2015) Poly(glycidyl methacrylate)-grafted clay nanofiller for highly transparent and mechanically robust epoxy composites. *Eur Polym J* 72:89–101
26. Monzo A, Rejtar T, Guttman A (2009) Optimization of poly(GMA-co-EDMA) monolithic support for trypsin nanoreactor fabrication. *J Chromatogr Sci* 47:467–472
27. Naidu P.S.R, Norret M, Dunlop S.A, Fitzgerald M, Clemons T.D, Iyer K.S (2019) Novel hydrophilic copolymer-based nanoparticle enhances the therapeutic efficiency of doxorubicin in cultured MCF-7 cells: *ACS Omega* 4:17083–17089.
28. Arshady R, Ledwith A, (the late), (1981) G.W. Kenner, Phenolic resins for peptide-synthesis. 2. Reactivities of phenolic and amino functional-groups in styrene based resins. *Macromol Chem Phy* 182:41–46
29. Ham G (1989) “Copolymerization, High Polymers”: Interscience: New York 18
30. Shiomi T, Suzuki M, Tohyama M, Imai K (1989) Dependence of miscibility on copolymer composition for blends of poly(vinylchloride-co-vinyl acetate) and poly(n-butyl methacrylate-co-isobutyl methacrylate): *Macromolecules* 22:3578–3581
31. Bednarski R, Braun D, Borbely J, Kelen T (1990) Copolymerization of styrene and methyl alpha-Cyanocinnamate, 1. Synthesis, NMR-Assignment, reactivity ratios. *Makromol Chem* 191:773–782
32. Chang TC, Wu KH, Chen HB, Ho SY, Chiu YS (1996) Thermal degradation of aged polytetrahydrofuran and its copolymers with 3-azidomethyl-3'-methyloxetane and 3-nitratomethyl-3'-methyloxetane by thermogravimetry. *J Polym Sci Part A Polym Chem* 34:3337–3343
33. Chang TC, Chen HB, Chiu YS, Ho SY (1997) Degradation of polydimethylsiloxane-block-polystyrene copolymer. *Polym Degrad Stab* 57:7–14
34. Miao L, Xu L, Narducy KW, Trudell ML (2009) First multigram preparation of SCP-123, a novel water-soluble analgesic. *Org Process Res Dev* 13:820–822
35. Fineman M, Ross SD (1950) Linear method for determining monomer reactivity ratios in copolymerization. *J Polym Sci* 5:259–262
36. Kelen T, Tudos F (1974) Analysis of the linear methods for determining copolymerization reactivity ratios. I. A new improved linear graphical method. *J Mac Sci Part A-Chem* 9:1–27
37. Connerton IF (1994) In *Analysis of Membrane Proteins*, Ed by Gould G.W.: Portland, London, 177
38. Chan ECZ, Pelczar MJ, Krieg NR (1993) *Agar Diffusion Method, in Laboratory Exercises in Microbiology*, ed by Chan, et all, McGraw-Hill: New York, 225
39. Melville HW, Noble B, Watson WF (1949) Copolymerization. II. Molecular weight distribution and mean molecular weights in copolymerization systems. *J Polym Sci* 4:629–637
40. Cheng S, Zhang M, Dixit N, Moore RB, Long TE (2012) Nucleobase self-assembly in supramolecular adhesives. *Macromolecules* 45:805–812
41. Heinzmann C, Weder C, de Espinosa CLM (2016) Supramolecular polymer adhesives: advanced materials inspired by nature. *Chem Soc Rev* 45:342–358
42. Diñçer S, Köseli V, Kesim H, Rzaev ZMO, Pişkin E (2002) Radical copolymerization of N-isopropylacrylamide with anhydrides of maleic and citraconic acids. *Eur Polym J* 38:2143–2152
43. Ham G (1964) *Copolymerization, High Polymers*. Interscience, New York
44. Botta A, de Candia F, Palumbo R (1985) Glass transition in aliphatic polyamides. *J Appl Polym Sci* 30:1669–1677
45. Di Marzio EA, Gibbs JH (1963) Molecular interpretation of glass temperature depression by plasticizers. *J Polym Sci A: Gen Papers* 1:1417–1428
46. Fox Jr TG, Flory PJ (1950) Second order transition temperatures and related properties of polystyrene. I. Influence of molecular weight. *J Appl Phys* 21:581
47. Coskun M, Erol I, Coskun MF, Demirelli K (2002) Thermal degradation behaviour of two methacrylate polymers with side chain amide groups. *Polym Degrad Stab* 78:49–55
48. Coskun M, Demirelli K, Erol I, Ahmedzade M (1998) Thermal degradation of poly [2-(3-aryl-3-methylcyclobutyl)-2-hydroxyethyl methacrylate]. *Polym Degrad Stab* 61:493–497
49. Erol I, Soykan C, Ilter Z et al (2003) Thermal degradation of poly 2-[3-(6-tetralino)-3-methylcyclobutyl]-2-ketoethyl methacrylate. *Polym Degrad Stab* 81:287–295
50. Takeo O (1965) A new method of analyzing thermogravimetric data. *Bull Chem Soc Jpn* 38:1881–1886
51. Regnier N, Guibe C (1997) Methodology for multistage degradation of polyimide polymer. *Polym Degrad Stab* 55:165–172
52. Kissinger HE (1957) Reaction kinetics in differential thermal analysis. *Anal Chem* 29:1702–1706
53. Farhoosh R, Johnny S, Asnaashari M, Molaahmadibahraseman N, Sharif A (2016) Structure-AA relationships of *o*-hydroxyl, *o*-methoxy, and alkyl ester derivatives of *p*-hydroxybenzoic acid. *Food Chem* 194:128–134
54. Siquet C, Paiva-Martins F, Lima JLFC, Reis S, Borges F (2006) Antioxidant profile of dihydroxy- and trihydroxyphenolic acids—a structure-activity relationship study. *Free Radical Res* 40:433–442
55. Muñoz-Bonilla A, Fernández-García M (2012) Polymeric materials with antimicrobial activity. *Prog Polym Sci* 37:281–339
56. Lorenzo CA, Concheiro A, Dubovik AS, Grinberg NV, Burova TV, Grinberg VY (2005) Temperature-sensitive chitosan-poly(N-isopropylacrylamide) interpenetrated network with enhanced loading capacity and controlled release properties. *J Control Release* 102:629–641
57. Tasdelen B, Apohan NK, Guven O, Baysal BM (2004) Preparation of poly(N-isopropylacrylamide/itaconic acid) copolymeric hydrogels and their drug release behavior. *Int J Pharm* 278:343–351
58. Sen M, Yakar A (2001) Controlled release of antifungal drug terbinafine hydrochloride from poly(N-vinyl 2-pyrrolidone/itaconic acid) hydrogels. *Int J Pharm* 228:33–41